UNIVERSITY *of York*

This is a repository copy of *An Experimental Investigation on Output Power Enhancement with Offline Reconfiguration for Non-Uniform Aging Photovoltaic Array to Maximise Economic Benefit*.

Article:

Takedown

White Rose
university consortium
Universities of Leeds, Sheffield & York

eprints@whiterose.ac.uk
https://eprints.whiterose.ac.uk/

An Experimental Investigation on Output Power Enhancement With Offline Reconfiguration for Non-Uniform Aging Photovoltaic Array to Maximise Economic Benefit

MOHAMMED ALKAHTANI [1], (Graduate Student Member, IEEE), **JIAFENG ZHOU** [1], **YIHUA HU** [2], (Senior Member, IEEE), **FAHAD ALKASMOUL** [3], **ZERYAB HASSAN KIANI** [4], **AND COLIN SOKOL KUKA** [2], (Graduate Student Member, IEEE)

[1] Department of Electrical and Engineering, University of Liverpool, Liverpool L69 3GJ, U.K.
[2] Department of Electronic Engineering, University of York, York YO10 5DD, U.K.
[3] Department of National Centre for Air Conditioning, King Abdulaziz City for Science and Technology (KACST), Riyadh 12354, Saudi Arabia
[4] Department of Manager Projects and Data Analytics, Sun In Motion LLC, Dubai, United Arab Emirates

Corresponding author: Colin Sokol Kuka (sk1759@york.ac.uk)

ABSTRACT There are several non-uniform effects on photovoltaic (PV) modules related to aging in a PV array. These subsequently bring about non-uniform operating parameters with individual PV modules, causing a variance in the PV array performance. The current study undertakes an indoor experimental study to establish and positively affect the efficacy of a non-uniform aged 2×4 PV array, with a commercially available small panel module of 0.36W (monocrystalline). This paper proposes a gene evolution algorithm (GEA) for offline reconfiguration that can provide more significant output power compared to non-uniformly aged PV arrays through repositioning instead of replacing aged PV modules, which will help lower maintenance expenses. This reconfiguration requires data input from the PV module's electrical properties in order to select ideal reconfiguration setups. The outcomes show that greater output power can be facilitated through a non-uniformly aged PV array and used on many different PV array sizes.

INDEX TERMS Solar photovoltaic, rearrangement, offline reconfiguration, non-uniform aging, gene evaluation algorithm, output characteristics.

I. INTRODUCTION

Energy resources and demand are critical to the development of emerging economies and their long-term viability. Fossil fuels are the main fuel source for the world economy needs, but these resources are finite and are rapidly running out, therefore bringing negative impacts on the wider ecosystem. Worldwide energy consumption has increased by 3000% in the 21st century alone, and the lack of sustainable resources is becoming increasingly apparent. As energy needs are increasing, the negative impacts seen in the environment are also rising. Greenhouse gases are released into the environment through heavy carbon fuels, facilitating dangerous climate

The associate editor coordinating the review of this manuscript and approving it for publication was Geng-Ming Jiang.

change. In turn, there is a pressing need to find a renewable energy source that does not produce pollution in order to meet current world needs. The energy provided by the sun can be exploited in different ways, such as photovoltaic (PV) processing, which uses the sun's energy to produce electricity. Through PV panels, sunlight is transformed into energy, and solar energy is consistently rising in popularity and applicability as alternative green energy compared to traditional energy-producing methods. On the other hand, PV device performance is highly related to levels of shading.

With regards to electrical characteristics, the selected PV modules in an array were confirmed as identical. There are unique changes in these modules when working under inhomogeneous insolation, which facilitates mismatch losses in a PV system and brings PV aging. In relation to efficiency

and energy yield, a PV system's design needs assessment of operation in a wide range of atmospheric conditions, such as shadow, dust, bird droppings, cracks and more. Aging also influences the energy yield and electrical performance of a PV system, and if this is substantial, then the system will not achieve its potential payback point [1]. Because of environmental conditions, the I-V curves produced change from their standard form, and there is a significant drop in PV array output power as a result [2], [3]. In large solar PV arrays, aging caused by environmental factors is a significant problem. The impact of environmental conditions on a solar PV system's power output has been widely investigated in other studies [4], [5].

Similarly, power output losses as a result of aging has also received significant study focus [6]–[9]. Based on environmental conditions, there is the possibility that many local maximum power point (MPP) will become apparent. In turn, the efficient tracking of global MPP is restricted by these local MPP, causing poor overall performance, hot spots being created and premature cell and module degradation [10], [11].

To make sure optimal performance is achieved, and mismatch losses of a PV system are limited (under aging conditions), a number of interconnection configurations have been suggested for PV modules [12]–[15]. Numerous simulation studies for various interconnection setups for PV modules were undertaken in order to examine PV module electrical behavior [16]–[18]. Besides, refs have compared basic interconnection schemes series and parallel configuration (SP) and their impact on bypass diodes. [19]–[21]. It was shown that the power loss in series-connected PV modules under mismatching was able to be mitigated with anti-parallel bypass diodes [22], [23]. Furthermore, there was a greater effect seen by the parallel configuration under mismatching [18], [24], [25]. There is a clear need for an optimal power conditioning system together with a suitable DC-DC converter when it comes to controlling a high current output at a low voltage level in parallel interconnection schemes [26]–[28]. Earlier literature has shown a range of different interconnection schemes, including series-parallel (SP), Total-cross-tied (TCT), Bridge-linked (BL) and Honeycomb configuration (HC), depicted in Figure 1. In refs [28]–[30] an optimal Sudoku configuration was presented, which had the disadvantages of a complicated configuration due to a large increase in the wiring. Piccoli *et al.* [31] put forward a different approach, which would more efficiently use building-integrated PV (BIPV) systems. A virtual reality environment was used when analysing the PV modules and nearby obstacles, but this did not offer any additional insight into the impacts of real-time problems related to various PV array configurations.

The study in [12], [13], [32], [33] developed an offline rearrangement approach in order to increase the energy efficiency of aged PV systems by examining potential rearrangements made to PV modules in line with maximum power point (MPP). Besides, [34] used the Munkres algorithm to evaluate optimal arrangement for balancing and
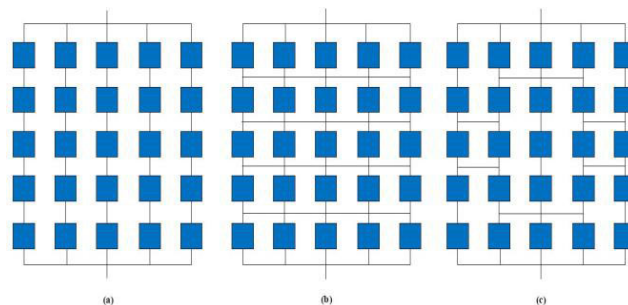
FIGURE 1. Twenty-five PV panels are interconnected in (a) SP; (b) TCT; (c) BL configurations.

attenuating the switches' aging process in the switching matrix [35], [36]. Problems concerning different sized PV array module restructuring were shown to be managed effectively under other methods. On the other hand, these are highly complicated from a computational standpoint and very time-consuming, as there is a need to search for every possible restructuring option [13], [37].

The current paper intends to suggest a way to reposition aging PV modules in such a way that the PV system has a less negative impact, using indoor experimentation. This will increase the power a PV array can produce, and for the current study needs, the algorithm can quickly find the optimal reconfiguration. The paper structure is as follows: Section II Methodology defines the developed reconfiguration scheme for a non-uniformly aged PV array. Section III presents the simulation and the experimental findings concerning the 2×4 PV arrays. Section IV includes a discussion of these findings, while Section V describes this study's conclusions.

II. METHODOLOGY
A. PV MODULE CHARACTERISTICS
This experiment used a 2×4 PV array to assess the efficiency of different array interconnection topologies for reducing mismatch loss due to aging factors. In turn, eight polycrystalline small PV modules (0.36 W/m^2 and 25°C) were used as shown in Figure 2, and the electrical specifications of single PV modules are clearly in Table 1 and Figure 3 [38]. Because of the current pandemic (COVID-19), the experiment was performed at home in an indoor laboratory. Five different aging patterns were employed to effectively analyses the performance when linked in a series-parallel SP topology. The details of array configuration, aging patterns, and detail experimental procedure are described in the following subsections.

B. PV ARRAY CONFIGURATION
The current paper examines SP topology due to its theoretical potential of being retrofitted effectively in all current PV fields. It is considered that almost all SP topology reconfiguration examinations have been completed through an examination of PV units. These PV units can be depicted simplistically, with strings of PV cells. Also, the fact that multiple maxima in the P-V features of several strings of

FIGURE 2. The type of small solar power panel 0.36W 2V Polycrystalline SunPower DIY module.

TABLE 1. Electrical specification of monocrystalline ANYSOLAR Ltd (SM301K09L-ND) module and array.

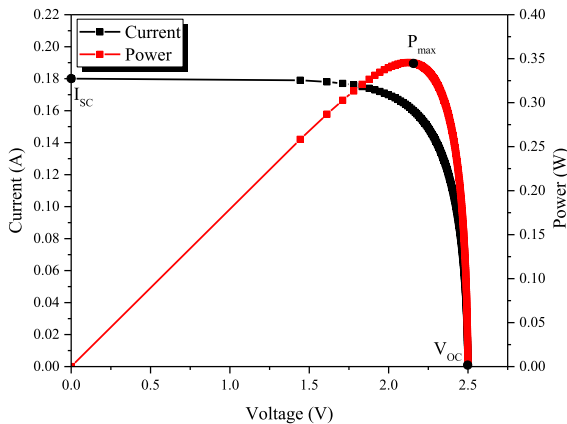| Parameter	Unit	Symbol	PV module (8 Cell)
Open Circuit Voltage	V	V_{OC}	2.5
Short Circuit Current	A	I_{SC}	0.180
Maximum Power Point Voltage	V	V_{mpp}	2
Maximum Power Point Current	A	I_{mpp}	0.160
Maximum Power Point	W	P_{mpp}	0.36
Operating Temperature	T	°C	25

FIGURE 3. Magnetization I-V and P-V curves of single PV (At standard test conditions) of the healthy module.

this kind could be present must be accounted for as well. When it comes to commercially available PV modules, cell strings are protected through a dedicated bypass diode paired with an aging factor, impacting the module. Frequently, this brings about several maximum power point tracking (MPP) conditions. Notably, most studies focusing on TCT architecture reconfiguration algorithms do not take into account the multi-modality of P-V curves [16], [39], [40].

Furthermore, short-circuit currents were investigated almost exclusively in all existing studies. In turn, the current paper analyses a reconfiguration algorithm for the SP connection of commercially available PV modules instead,
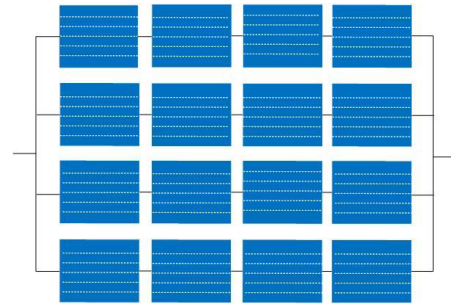

FIGURE 4. Sixteen PV panels are interconnected in Series-Parallel (SP) configuration.

(a) Aging pattern - I (b) Aging pattern - II

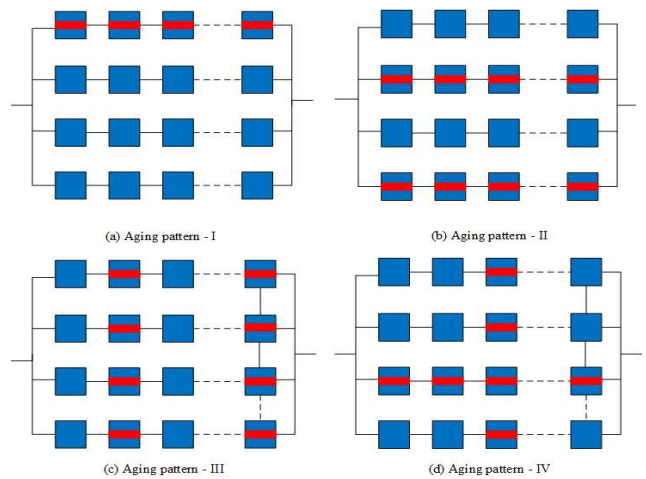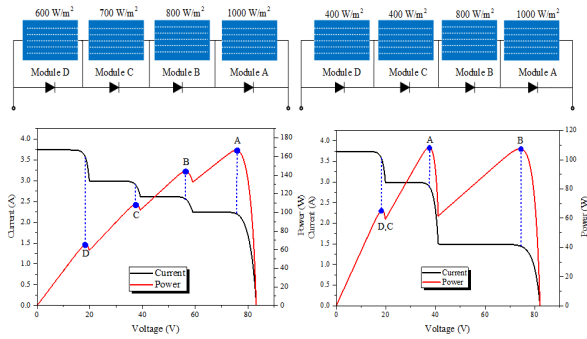(c) Aging pattern - III (d) Aging pattern - IV

FIGURE 5. Four different PV modules aging patterns for SP configuration (a, b, c and d).

based on comprehending the entire I-V characteristic range of each PV module. This way, the reconfiguration algorithm can accurately describe the prevalence of maximum power point (MPP) in different PV modules' P-V features. It should also be noted that the current study intends to develop an SP reconfiguration strategy that can be used in faulty PV modules as seen in Figure 4, or those with defective or aging PV systems, instead of simply comparing SP and TCT topology reconfiguration performances. This way, a PV array's maximum power output can be boosted by changing the PV module positions. The suggested algorithm needs to establish the optimal configuration rapidly and then apply it in polynomial time.

C. PV ARRAY AGING PATTERNS
An example, random 16 PV modules connected in the PV string series for medium size PV array are commonly used for the MPPT investigation. Besides, PV module aging is achieved through films, and Figure 5 shows the suggested aging patterns, which can be used as examples of the SP configuration. In aging pattern-I, (a) four modules are aging (in the first string) horizontally. In aging pattern-II, (b) two strings are aging as (a) horizontally. Finally, in aging pattern-III, (c) eight modules are aging vertically, and the

FIGURE 6. Example of connecting PV panels/module in series and parallel, where the healthy module begins 1000W/m².

modules are connected in parallel. This type of aging technique was employed on eight modules in order to produce aging pattern-IV, (d). These aging patterns' significance is evaluated using array current, array voltage, and power for the array configuration SP. As a result, Figure 6 shows the first PV string of pattern-I (a) as an example with three peaks in the top right corner and two PV modules (D and C) with ageing patterns for P–V curves. Simultaneously, the PV string in the top left identified four different ageing of second patterns-II, (b), with modules (D and C) exhibiting ageing factors. In contrast, the others (B and A) remained stable.

D. RECONFIGURATION BEASED ON GENE EVOLUTION ALGORTHIM

Based on GEA, the configuration that generates the most power out of all possible connection patterns with the lowest total number of PV module substitutions can be found. This algorithm's advantages include its ability to conduct an arbitrary local search (to an extent). Simultaneously, mutation processes can accelerate convergence to a better solution once the iteration is close to a superior solution at a given number of times. Besides, precocity is reduced through the availability of numerous practical solutions. For GEA applications, it is necessary to represent each configuration using a row of numbers as a chromosome while estimating each configuration's power output using a fitness function. Pre-prepared chromosomes make up the fitness function inputs, and, in turn, the GEA uses the results to establish the chromosomes selected as parents for the future generation of chromosomes [13], [41]. Therefore, an on and off switching of the GEA-computed PV array module is needed, along with the lowest number of substitutions.

$$PV = \frac{pv_w}{\sum\limits_{j-1}^{n_{pv}} s_{n(j)} v_{oc}} \tag{1}$$

$$j = 1, 2, \ldots, n \times m \tag{2}$$

where S_n is the module short-circuit current, V_{oc} is the open-circuit voltage; PV power is the power delivered by the PV array, and n_{pv} is the number of modules in the system.

TABLE 2. The steps of SP configuration by using the gene evolution algorithm.

	Parameters	Function
I.	Fitness	Equations (1 and 2) express the proposed fitness function, and the GEA is intended to maximise the PV value to the maximum power.
II.	Parametric Design	1. Population size = 300 2. Chromosome Length = $n \times m$ 3. Evolution time = 3000
III.	Decimal-Based Encoding	Direct coding with the PV module number; hence, a sequence will take the form of chromosome expression.
IV.	Evaluate the Fitness of Each Chromosome in Population	PV estimation is performed based on the formulated fitness function after chromosome mapping into a two-dimensional array n×m.
V.	Achieving Iterations Objective	Steps VI-VII, for example, can only be bypassed if the evaluation succeeds.
VI.	Selection of Parents for The Future Generation	This means sorting the fitness from large too small to identify the surviving chromosome, followed by a random number of individuals who survive despite low fitness.
VII.	Parental Chromosome Crossover	This issue is challenging due to the crossover approach; a sequential hybridisation algorithm is used. An exchange of hybridisation segments and the parental models' relative positions help determine the other positions.

Thus, GEA intends to maximise the PV value, as shown in Table 2.

To explain part (VII) in Table 2. The other positions are determined based on the relative positions of the models of the parents. For example, the chromosome can be given as the sequence {1,2,3...,8}.

$$n \times m = \begin{bmatrix} PV_{11} & PV_{12} & PV_{13} & PV_{14} \\ PV_{21} & PV_{22} & PV_{23} & PV_{24} \end{bmatrix} \tag{3}$$

Assume:

$$Parent_{one} = \{8, 6, 3, 5, 4, 1, 7, 2\} \tag{4}$$

$$Parent_{two} = \{1, 7, 8, 2, 5, 6, 4, 3\} \tag{5}$$

Then, the random hybridisation points selected from parent one = {8,6,3,5,4,1,7,2} and in parent two = {1,7,8,2,5,6,4,3}.

In order to swap the hybrids:

$$Parent_{one} = \{\#, \#, \#, |2, 5, 6|, \#, \#\} \tag{6}$$

$$Parent_{two} = \{\#, \#, \#, |5, 4, 1|, \#, \#\} \tag{7}$$

And then, get to the group from the second hybridisation point of parents one in equations (4 and 5) and removing the elements in the hybridisation segment {2, 5, 6}, finally getting the {8, 3, 4,1,7},
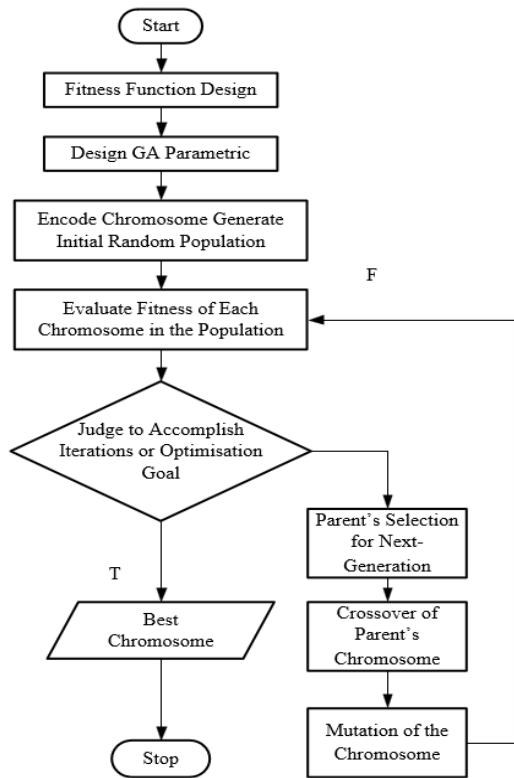
FIGURE 7. Displayed the flow chart of GEA procedure of PV array reconfiguration.

Thus, the outcome in parent one for hybridization point 6 from the second crossing point in turn:

$$Parent_{one} = \{4, 1, 7, \|2, 5, 6\|, 8, 3\} \qquad (8)$$

Similar,

$$Parent_{two} = \{7, 8, 2, \|5, 4, 1\|, 6, 3\} \qquad (9)$$

In this step, the chromosome Mutation scheme of three integers guarantees a certain population of mutations by choosing three specific mutations from within the population ($1 < u < v < w < n \times m$) and the genes between v and u, including u and v, with paragraph insertion after w; the fourth step is subsequently undertaken.

In the final step, the outputs of the chromosome, an overview of each configuration that satisfies every step and a possible initial state are given in Figure 4.

However, GEA found nine iterations enough to achieve optimal reconfiguration for a 2 × 4 PV array with heterogeneous aging. In Figure 7, the final step is shown together with the lowest swap times and the most significant output power. Algorithm code used in Python 3.6.2 Intel (R) Core (7M) i7-8565u CPU @1.80 GHz/Windows 10/8 GB/512GB SSD/UHD 620 to be a suitable computer with which to find the ideal configuration for a sizable PV array.

E. EXPEREMNTAL STUDY

This section discusses the research setup and measurement processes. The experiment involved 2 × 4 arrays in
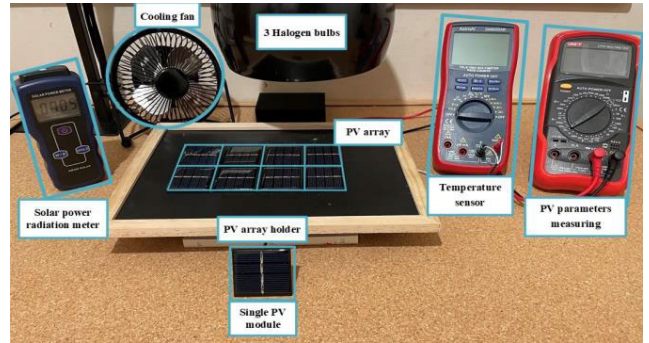

FIGURE 8. Experimental prototype to investigate before and after arranging the I-V and P-V characteristics of the PV array by offline reconfiguration.

TABLE 3. The output of the I-V tracer parameters.

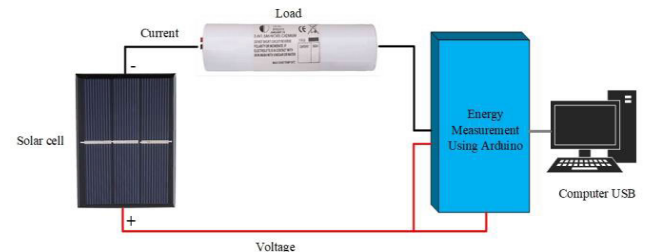| I-V Parameters	Accuracy of Measurement	Range of Measurement
Voltage measurement (V)	±1%	7.5-7.8
Current measurement (A)	±1%	0.170-0.174
Temperature (°C)	±2%	+25 to +50
Irradiance (W/m^2)	±3%	0-1200

FIGURE 9. Experimental setup to investigate the I-V and P-V characteristics of the single module and array.

confirming the suggested approach, depending on availability. In Figure 8, three halogen bulbs are employed as artificial sunlight (0.5kW each), positioned parallel to the display modules. Practical used flexible wires and clips to link the individual PV modules' output edges to make the connections more manageable. In turn, commercial multimeters were used to evaluate the PV array's output I−V and P−V parameters, along with an irradiance sensor and temperature sensor. The room temperature was 25°C during the experiment, with a variable speed cooling fan used.

Following the experiment, the results are shown in the III below.

Furthermore, the setup of this experiment identifies the requirements for describing as illustrated in Figure 9 to obtain the performance characteristics of PV single and array modules below:

- As in the full sun, a solar cell is positioned at a fixed distance from a light source (using artificial sunlight).
- The voltage probe was connected to the solar cell's output, with the black lead to the negative and the red lead to the positive.

TABLE 4. The output of the Current (I)-Voltage (v) tracer parameters.

PV cell parameters	Values	Units
Voltage Cell	2.27	V
Current Cell	0.16	A
Power Cell	0.36	W
Voltage Array	18.16	V
Current Array	0.16	A
Power Array	2.91	W

TABLE 5. A 2 × 4 PV array before reconfiguration.

The PV age module condition (per unit)				
0.7 p.u.	1 p.u.	0.5 p.u.	1 p.u.	Row (string 1)
1 p.u.	0.6 p.u.	0.9 p.u.	0.5 p.u.	Row (string 2)

TABLE 6. PV array 2 × 4 output parameters before reconfiguration.

Parameters	Parameters	Parameters
Voltage	7.8	V
Current	0.174	A
Power	1.498	W

- The current probe was connected in series with a battery load to the solar cell's output.
- Figure 3 displayed the I-V and P-V using Python MPP code and store output data.
- In a PV array, the measurement was repeated with a different solar cell.
- The calculation was repeated with different illumination levels, to get the best results, such as changing the artificial sunlight.

Following the experiment, the results of the healthy PV modules are shown in Table 4 below.

III. ANALYSIS OF THE RESULTS

A. 2 × 4 PV ARRAY BEFORE REARRANGEMENT

Table 4 shows the exact PV module parameters in the experiment. A plastic cling film is used to cover the four modules positioned in both two strings (module11, module13, module22, module23 and module24) illustrated in Figure 10 in order to achieve the aging condition. The maximum short-circuits currents in a healthy module are set as per unit (1 p.u.), from standard test conditions STC (1000 W/m^2) at 25 °C module temperature. Figure 11 shows the test results seen before the arrangement, with the module output characteristics for both strings shown in Table 5.

Before applying the suggested PV array method, and I-V and P-V were not reconfigured, the PV array maximum output power was 1.498 W. The voltage was 7.8 V, and the current was 0.174 A respectively, as depicted in Table 6, and Figure 12 describes the final parameters before rearrangement.

B. 2 × 4 PV ARRAY AFTER REARRANGEMENT

Once the suggested strategy is used on the PV array, nine iterations were used to define the optimal reconfiguration
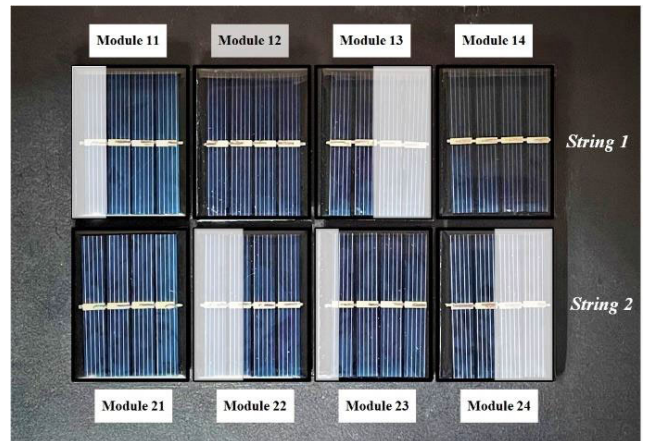
FIGURE 10. The non-uniform aging PV modules without reconfiguration (covered with a black plastic membrane).
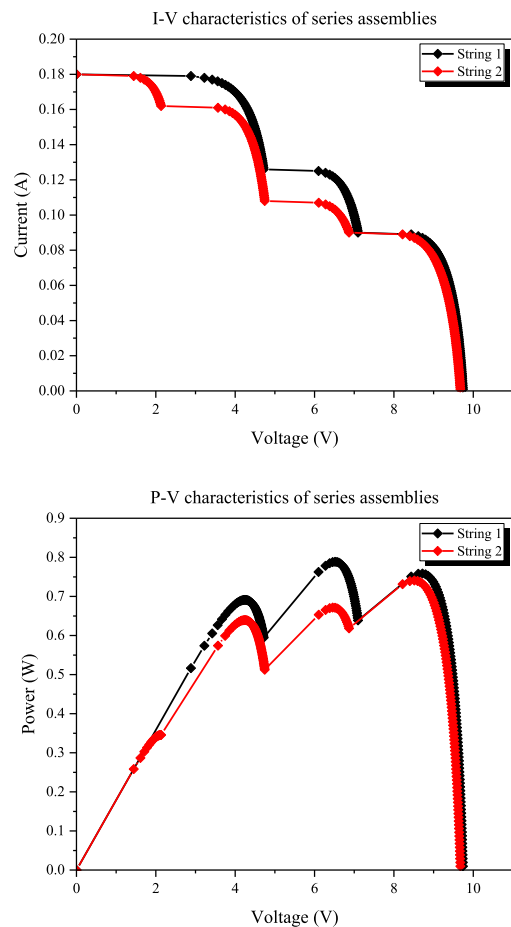
FIGURE 11. The 2 × 4 PV modules output characteristics of I-V and P-V before reconfiguration.

for a 2 × 4 PV array with heterogeneous aging, as depicted in Table 7. Figure 7 describes the last stage, with the smallest amount of swap times illustrated in Figure 13, as well as increasing the output power.

Identifying the optimal reconfiguration allowed the final stage to be reached through greater output power and reduced swap to the greatest degree. Thus, the ideal PV modules
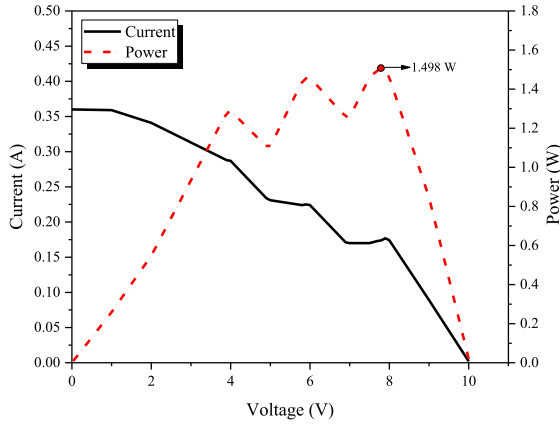
FIGURE 12. The outputs of the 2 × 4 PV array (before rearrangement).

```
0.5 row 1, col 1 is swapped by 1.0  row 4, col 2
0.9 row 1, col 2 is swapped by 0.5  row 4, col 1
0.6 row 2, col 1 is swapped by 1.0  row 3, col 2
0.7 row 2, col 2 is swapped by 1.0  row 3, col 1
1.0 row 3, col 1 is swapped by 0.7  row 2, col 2
1.0 row 3, col 2 is swapped by 0.6  row 2, col 1
0.5 row 4, col 1 is swapped by 0.9  row 1, col 2
1.0 row 4, col 2 is swapped by 0.5  row 1, col 1

Total swaps: 8
>>>
```

FIGURE 13. Final iterations to obtain the ideal configuration for the proposed method.

TABLE 7. A 2 × 4 PV array after reconfiguration.

The PV age module condition (per unit)				
1 p.u.	0.5 p.u.	1 p.u.	1 p.u.	**Row (string 1)**
0.7 p.u.	0.6 p.u.	0.9 p.u.	0.5 p.u.	**Row (string 2)**

were replaced with ones that could boost final output power, described with:

- (PV module11 in string 1 "swapped" with PV module21 in string 2).
- (PV module12 in string 1 "swapped" with PV module13 in string 2).

This shows that the reconfiguration established the lowest swap times where only four PV modules shifted position to boost output power, while the others (module14, module22, module23 and module24) did not move, as seen in Figure 14. In addition, the PV module output properties of I-V and P-V after reconfiguration are depicted in Figure 15 as a series connection.

Once the suggested PV array solution was applied, the algorithm's potential to uncover the optimal arrangement was ensured through simulating the two PV structures. The peak power output following rearrangement is shown in Figure 16, which was 1.669 W, with a PV array output voltage of 6 V and an MPP current of 0.258 A. The computational time for the suggested algorithm for describing aged 2 × 4 PV array rearrangements are shown in Table 8.

TABLE 8. PV array 2 × 4 output parameters after reconfiguration.

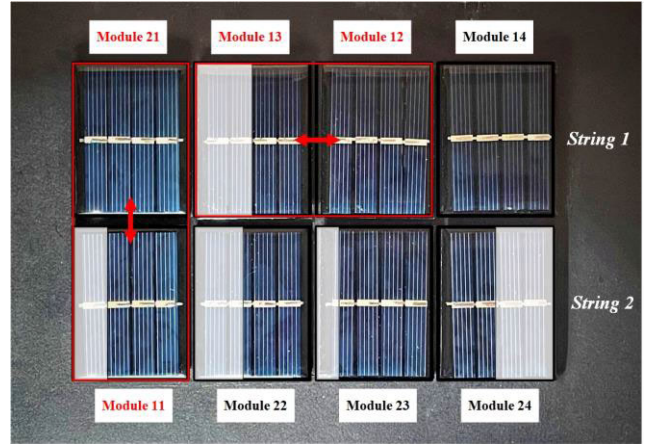| *Parameters*	*Parameters*	*Parameters*
Voltage	6	V
Current	0.258	A
Power	1.669	W

FIGURE 14. The non-uniform aging PV modules with reconfiguration (where 4 modules have swapped marked with red boxes).
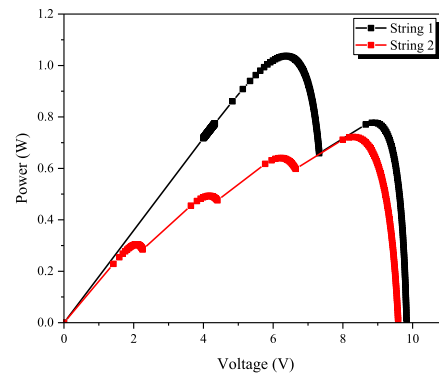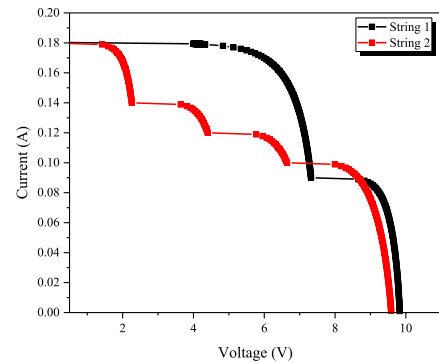

FIGURE 15. The series 2 × 4 PV modules output characteristics of I-V and P-V after reconfiguration.

IV. DISSECTION

For PV arrays of varying dimensions, the proposed algorithm can be applied to support maximum power output. Besides, for the 2 × 4 PV arrays, the algorithm considered important aging factors for rearranging specific PV module
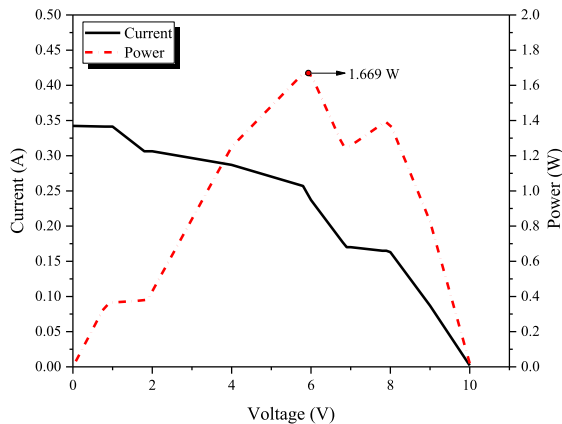
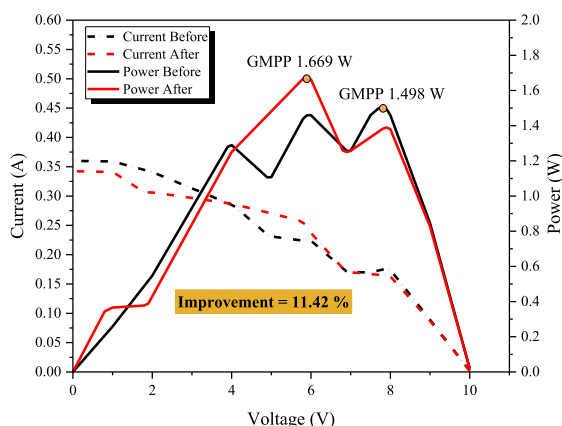**FIGURE 16.** The outputs of the 2 × 4 PV array (after rearrangement).

FIGURE 17. The outputs of PV arrays before and after arrangements, including a percentage of improvement.

positions in each string, therefore enhancing the impact of bypass diodes. In turn, all string PV modules suffered from mismatch loss to a smaller degree, but voltage limits were not considered. Additional studies which examine this area can be found [2], [33], [42]. The recommended algorithm has the ability to sort the PV modules iteratively and hierarchically. The produced P–V curves seen in Figure 17 depict the PV array reconfiguration strategy's potential to increase system efficiency and lower operating costs.

Besides, the proposed algorithm can bring about rapid results, as there is no requirement to access all potential configurations of a specific PV Array (Online or Offline), which streamlines the action. This was seen where the algorithm established the ideal PV module configuration in only nine steps, with an average computational time of 0.134325 s. Therefore, by finding an ideal module configuration quickly, the real-time implementation process is sped up. Another benefit of the proposed algorithm is that it only rearranges impacted PV modules, with others not being affected. Also, this paper shows that rearrangement increases maintenance management efficiency. Notably, expenditures and benefits are the critical decision criteria for offline reconfiguration methods. The selected methods increase reconfiguration efficiency, profitability, and cost-effectiveness during operation,

as developing an aging map for PV plants is crucial. Reconfiguration can be supported as a step towards maximising PV plant strengths once profitability and more outstanding power production outweigh the expense of labor force rearrangement. Once these elements are taken into account, the proposed methodology would provide many benefits. PV module positions would be replaced in line with the workforce instead of replacing all aging modules with new ones [41], [42].

V. CONCLUSION

The current paper concentrates on non-uniform aging processes in PV arrays. The included experiment presents the finding that PV array power production is impacted by the position of aged PV modules in the PV arrays. Thus, the suggested algorithm for reconfiguring PV arrays will help limit the effect of PV arrays with non-uniform aging while boosting the amount of power produced while overcoming the need to replace aged PV modules. The algorithm arranges the PV modules repetitively and hierarchically to mitigate the incompatibility effect of non-uniform aging amongst PV modules. In turn, the output power increased by 11.42 % for the 2 × 4 PV array, shown in Figure 17.

Therefore, the proposed approach for the offline reconfiguration of PV modules can raise the maximum power output of PV systems with more miniature relays than the online PV array reconfiguration approaches. The optimal reconfiguration strategy is determined by the costs and benefits involved. Finding the ageing map of a PV plant is needed to devise a cost-effective reconfiguration strategy that will also increase income. The swapping cost of PV modules relating to the workforce should also be found. By comparing the above values, the PV plant owner can decide whether to undertake the suggested reconfiguration if the increase in profit through more significant power generation surpasses the workforce's efforts in this regard. Thus, the suggested strategy's main benefit is to suggest suitable swaps of PV modules' positions only through a workforce.

REFERENCES

[1] A. Mansur, M. Amin, and K. Islam, "Performance comparison of mismatch power loss minimization techniques in series-parallel PV array configurations," *Energies*, vol. 12, no. 5, p. 874, Mar. 2019, doi: 10.3390/en12050874.

[2] G. Sai Krishna and T. Moger, "Reconfiguration strategies for reducing partial shading effects in photovoltaic arrays: State of the art," *Sol. Energy*, vol. 182, pp. 429–452, Apr. 2019, doi: 10.1016/j.solener.2019.02.057.

[3] R. Pachauri, R. Singh, A. Gehlot, R. Samakaria, and S. Choudhury, "Experimental analysis to extract maximum power from PV array reconfiguration under partial shading conditions," *Eng. Sci. Technol., Int. J.*, vol. 22, no. 1, pp. 109–130, Feb. 2019, doi: 10.1016/j.jestch.2017.11.013.

[4] M. Jaszczur, J. Teneta, Q. Hassan, E. Majewska, and R. Hanus, "An experimental and numerical investigation of photovoltaic module temperature under varying environmental conditions," *Heat Transf. Eng.*, vol. 42, nos. 3–4, pp. 354–367, Feb. 2021, doi: 10.1080/01457632.2019.1699306.

[5] A. A. Hachicha, I. Al-Sawafta, and Z. Said, "Impact of dust on the performance of solar photovoltaic (PV) systems under United Arab emirates weather conditions," *Renew. Energy*, vol. 141, pp. 287–297, Oct. 2019, doi: 10.1016/j.renene.2019.04.004.

[6] A. Azizi, P.-O. Logerais, A. Omeiri, A. Amiar, A. Charki, O. Riou, F. Delaleux, and J.-F. Durastanti, "Impact of the aging of a photovoltaic module on the performance of a grid-connected system," *Sol. Energy*, vol. 174, pp. 445–454, Nov. 2018, doi: 10.1016/j.solener.2018.09.022.

[7] E. I. Batzelis, P. S. Georgilakis, and S. A. Papathanassiou, "Energy models for photovoltaic systems under partial shading conditions: A comprehensive review," *IET Renew. Power Gener.*, vol. 9, no. 4, pp. 340–349, May 2015, doi: 10.1049/iet-rpg.2014.0207.

[8] S. Killinger, D. Lingfors, Y.-M. Saint-Drenan, P. Moraitis, W. van Sark, J. Taylor, N. A. Engerer, and J. M. Bright, "On the search for representative characteristics of PV systems: Data collection and analysis of PV system azimuth, tilt, capacity, yield and shading," *Sol. Energy*, vol. 173, pp. 1087–1106, Oct. 2018, doi: 10.1016/j.solener.2018.08.051.

[9] R. J. Mustafa, M. R. Gomaa, M. Al-Dhaifallah, and H. Rezk, "Environmental impacts on the performance of solar photovoltaic systems," *Sustainability*, vol. 12, no. 2, p. 608, Jan. 2020, doi: 10.3390/su12020608.

[10] F. Belhachat and C. Larbes, "Comprehensive review on global maximum power point tracking techniques for PV systems subjected to partial shading conditions," *Sol. Energy*, vol. 183, pp. 476–500, May 2019, doi: 10.1016/j.solener.2019.03.045.

[11] M. Kermadi, Z. Salam, J. Ahmed, and E. M. Berkouk, "A high-performance global maximum power point tracker of PV system for rapidly changing partial shading conditions," *IEEE Trans. Ind. Electron.*, vol. 68, no. 3, pp. 2236–2245, Mar. 2021, doi: 10.1109/TIE.2020.2972456.

[12] M. Alkahtani, Z. Wu, C. S. Kuka, M. S. Alahammad, and K. Ni, "A novel PV array reconfiguration algorithm approach to optimising power generation across non-uniformly aged PV arrays by merely repositioning," *J Multidisciplinary Sci. J.*, vol. 3, no. 1, pp. 32–53, Feb. 2020, doi: 10.3390/j3010005.

[13] M. Alkahtani, Y. Hu, Z. Wu, C. S. Kuka, M. S. Alhammad, and C. Zhang, "Gene evaluation algorithm for reconfiguration of medium and large size photovoltaic arrays exhibiting non-uniform aging," *Energies*, vol. 13, no. 8, p. 1921, Apr. 2020. [Online]. Available: https://www.mdpi.com/1996-1073/13/8/1921

[14] G. Mostafaee and R. Ghandehari, "Power enhancement of photovoltaic arrays under partial shading conditions by a new dynamic reconfiguration method," *J. Energy Manage. Technol.*, vol. 4, no. 1, pp. 46–51, 2020, doi: 10.22109/jemt.2019.150205.1126.

[15] S. Gul, A. Ul Haq, M. Jalal, A. Anjum, and I. U. Khalil, "A unified approach for analysis of faults in different configurations of PV arrays and its impact on power grid," *Energies*, vol. 13, no. 1, p. 156, Dec. 2019, doi: 10.3390/en13010156.

[16] S. Malathy and R. Ramaprabha, "Comprehensive analysis on the role of array size and configuration on energy yield of photovoltaic systems under shaded conditions," *Renew. Sustain. Energy Rev.*, vol. 49, pp. 672–679, Sep. 2015, doi: 10.1016/j.rser.2015.04.165.

[17] B. Boumaaraf, H. Boumaaraf, M. E.-A. Slimani, S. Tchoketch_Kebir, M. S. Ait-cheikh, and K. Touafek, "Performance evaluation of a locally modified PV module to a PV/T solar collector under climatic conditions of semi-arid region," *Math. Comput. Simul.*, vol. 167, pp. 135–154, Jan. 2020, doi: 10.1016/j.matcom.2019.09.013.

[18] F. Belhachat and C. Larbes, "Modeling, analysis and comparison of solar photovoltaic array configurations under partial shading conditions," *Sol. Energy*, vol. 120, pp. 399–418, Oct. 2015, doi: 10.1016/j.solener.2015.07.039.

[19] G. P. A. and A. K. Saha, "Effects and performance indicators evaluation of PV array topologies on PV systems operation under partial shading conditions," in *Proc. Southern Afr. Universities Power Eng. Conf./Robot. Mechatronics/Pattern Recognit. Assoc. South Afr. (SAUPEC/RobMech/PRASA)*, Jan. 2019, pp. 322–327, doi: 10.1109/RoboMech.2019.8704823.

[20] A. A. Desai and S. Mikkili, "Modelling and analysis of PV configurations (alternate TCT-BL, total cross tied, series, series parallel, bridge linked and honey comb) to extract maximum power under partial shading conditions," *CSEE J. Power Energy Syst.*, early access, Aug. 19, 2020, doi: 10.17775/CSEEJPES.2020.00900.

[21] A. Jubaer, N.-A. Hadi, and T. M. F. Naim, "Modified series-parallel photovoltaic configuration to enhance efficiency under partial shading," *Int. J. Integr. Eng.*, vol. 11, no. 3, pp. 207–215, Sep. 2019.

[22] A. K. Tripathi, M. Aruna, and C. S. N. Murthy, "Performance of a PV panel under different shading strengths," *Int. J. Ambient Energy*, vol. 40, no. 3, pp. 248–253, Apr. 2019, doi: 10.1080/01430750.2017.1388839.

[23] P. K. Bonthagorla and S. Mikkili, "Optimal PV array configuration for extracting maximum power under partial shading conditions by mitigating mismatching power loss," *CSEE J. Power Energy Syst.*, early access, Apr. 6, 2020, doi: 10.17775/CSEEJPES.2019.02730.

[24] S. Pareek and R. Dahiya, "Enhanced power generation of partial shaded photovoltaic fields by forecasting the interconnection of modules," *Energy*, vol. 95, pp. 561–572, Jan. 2016, doi: 10.1016/j.energy.2015.12.036.

[25] C. Saiprakash, A. Mohapatra, B. Nayak, and S. R. Ghatak, "Analysis of partial shading effect on energy output of different solar PV array configurations," *Mater. Today, Proc.*, vol. 39, pp. 1905–1909, 2021, doi: 10.1016/j.matpr.2020.08.307.

[26] V. Karthikeyan, S. Kumaravel, and G. Gurukumar, "High step-up gain DC–DC converter with switched capacitor and regenerative boost configuration for solar PV applications," *IEEE Trans. Circuits Syst. II, Exp. Briefs*, vol. 66, no. 12, pp. 2022–2026, Dec. 2019, doi: 10.1109/TCSII.2019.2892144.

[27] S. P. Litrán, E. Durán, J. Semião, and R. S. Barroso, "Single-switch bipolar output DC–DC converter for photovoltaic application," *Electronics*, vol. 9, no. 7, p. 1171, Jul. 2020, doi: 10.3390/electronics9071171.

[28] S. Bana and R. P. Saini, "A mathematical modeling framework to evaluate the performance of single diode and double diode based SPV systems," *Energy Rep.*, vol. 2, pp. 171–187, Nov. 2016, doi: 10.1016/j.egyr.2016.06.004.

[29] I. Nasiruddin, S. Khatoon, M. F. Jalil, and R. C. Bansal, "Shade diffusion of partial shaded PV array by using odd-even structure," *Sol. Energy*, vol. 181, pp. 519–529, Mar. 2019, doi: 10.1016/j.solener.2019.01.076.

[30] S. G. Krishna and T. Moger, "Optimal SuDoKu reconfiguration technique for total-cross-tied PV array to increase power output under non-uniform irradiance," *IEEE Trans. Energy Convers.*, vol. 34, no. 4, pp. 1973–1984, Dec. 2019, doi: 10.1109/TEC.2019.2921625.

[31] E. Piccoli, A. Dama, A. Dolara, and S. Leva, "Experimental validation of a model for PV systems under partial shading for building integrated applications," *Sol. Energy*, vol. 183, pp. 356–370, May 2019, doi: 10.1016/j.solener.2019.03.015.

[32] Y. Hu, J. Zhang, P. Li, D. Yu, and L. Jiang, "Non-uniform aged modules reconfiguration for large-scale PV array," *IEEE Trans. Device Mater. Rel.*, vol. 17, no. 3, pp. 560–569, Sep. 2017, doi: 10.1109/TDMR.2017.2731850.

[33] Y. Hu, J. Zhang, J. Wu, W. Cao, G. Y. Tian, and J. L. Kirtley, "Efficiency improvement of nonuniformly aged PV arrays," *IEEE Trans. Power Electron.*, vol. 32, no. 2, pp. 1124–1137, Feb. 2017, doi: 10.1109/TPEL.2016.2544842.

[34] T. N. Ngoc, E. R. Sanseverino, N. N. Quang, P. Romano, F. Viola, B. D. Van, H. N. Huy, T. T. Trong, and Q. N. Phung, "A hierarchical architecture for increasing efficiency of large photovoltaic plants under non-homogeneous solar irradiation," *Sol. Energy*, vol. 188, pp. 1306–1319, Aug. 2019, doi: 10.1016/j.solener.2019.07.033.

[35] M. Manjunath, B. V. Reddy, and B. Lehman, "Performance improvement of dynamic PV array under partial shade conditions using M² algorithm," *IET Renew. Power Gener.*, vol. 13, no. 8, pp. 1239–1249, Jun. 2019, doi: 10.1049/iet-rpg.2018.5675.

[36] A. Tabanjat, M. Becherif, and D. Hissel, "Reconfiguration solution for shaded PV panels using switching control," *Renew. Energy*, vol. 82, pp. 4–13.

[37] P. Udenze, Y. Hu, H. Wen, X. Ye, and K. Ni, "A reconfiguration method for extracting maximum power from non-uniform aging solar panels," *Energies*, vol. 11, no. 10, p. 2743, Oct. 2018, doi: 10.3390/en11102743.

[38] PowerFilm. *Electronic Component Solar Panels*. PowerFilm, Inc. Accessed: Mar. 21, 2021. [Online]. Available: https://www.powerfilmsolar.com/products/electronic-component-solar-panels/classic-application-series/

[39] L. Cristaldi, M. Faifer, M. Rossi, S. Toscani, M. Catelani, L. Ciani, and M. Lazzaroni, "Simplified method for evaluating the effects of dust and aging on photovoltaic panels," *Measurement*, vol. 54, pp. 207–214, Aug. 2014, doi: 10.1016/j.measurement.2014.03.001.

[40] G. Velasco-Quesada, F. Guinjoan-Gispert, R. Pique-Lopez, M. Roman-Lumbreras, and A. Conesa-Roca, "Electrical PV array reconfiguration strategy for energy extraction improvement in grid-connected PV systems," *IEEE Trans. Ind. Electron.*, vol. 56, no. 11, pp. 4319–4331, Nov. 2009, doi: 10.1109/TIE.2009.2024664.

[41] M. Alkahtani, Y. Hu, M. A. Alghaseb, K. Elkhayat, C. S. Kuka, M. H. Abdelhafez, and A. Mesloub, "Investigating fourteen countries to maximum the economy benefit by using offline reconfiguration for medium scale PV array arrangements," *Energies*, vol. 14, no. 1, p. 59, Dec. 2020, doi: 10.3390/en14010059.

[42] Z. Wu, C. Zhang, M. Alkahtani, Y. Hu, and J. Zhang, "Cost effective offline reconfiguration for large-scale non-uniformly aging photovoltaic arrays efficiency enhancement," *IEEE Access*, vol. 8, pp. 80572–80581, 2020, doi: 10.1109/ACCESS.2020.2991089.

MOHAMMED ALKAHTANI (Graduate Student Member, IEEE) received the B.Eng. degree (Hons.) in electrical and electronics engineering and the M.Sc. degree in electrical power and control engineering from Liverpool John Moores University, Liverpool, U.K., in 2014 and 2016, respectively. He is currently pursuing the Ph.D. degree with the University of Liverpool. His research interests include the management of photovoltaic and a PV array efficiency improvement.

JIAFENG ZHOU received the B.Sc. degree in radio physics from Nanjing University, Nanjing, China, in 1997, and the Ph.D. degree from the University of Birmingham, Birmingham, U.K., in 2004, with a focus on high-temperature superconductor microwave filters.

Since July 1997, he has been with the National Meteorological Satellite Centre of China, Beijing, China, where he was involved with the development of communication systems for Chinese geostationary meteorological satellites. From August 2004 to April 2006, he was a Research Fellow with the University of Birmingham, where his research concerned phased arrays for reflector observing systems. Then he moved to the Department of Electronic and Electrical Engineering, University of Bristol, Bristol, U.K., until August 2013. His research in Bristol was on the development of highly efficient and linear amplifiers. He is currently with the Department of Electrical Engineering and Electronics, University of Liverpool, Liverpool, U.K. His current research interests include microwave power amplifiers, filters, metamaterials, other radio frequency devices, electromagnetics, wireless power transfer, and energy harvesting.
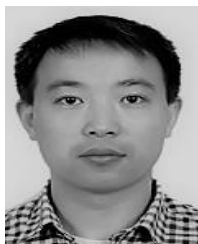
YIHUA HU (Senior Member, IEEE) received the B.S. degree in the electrical motor driver and the Ph.D. degree in power electronics and drives from the China University of Mining and Technology, Xuzhou, China, in 2003 and 2011, respectively. From 2011 to 2013, he was with the College of Electrical Engineering, Zhejiang University, as a Postdoctoral Fellow. From 2012 to 2013, he was an Academic Visiting Scholar with the School of Electrical and Electronic Engineering, Newcastle University, Newcastle upon Tyne, U.K. From 2013 to 2015, he was a Research Associate with the Power Electronics and Motor Drive Group, University of Strathclyde. He is currently a Lecturer with the Department of Electrical Engineering and Electronics, University of Liverpool. He has authored over 35 peer-reviewed technical articles in leading journals. His research interests include PV generation systems, power electronics converters and control, and electrical motor drives.

FAHAD ALKASMOUL received the B.S. and M.Sc. degrees in mechanical engineering from King Saud University (KSU), in 2000 and 2006, respectively, and the Ph.D. degree in heat transfer and computational fluid dynamic from the University of Leeds, England, in 2016. He is currently the Director of the National Centre for Air Conditioning, King Abdulaziz City for Science and Technology (KACST), Saudi Arabia. His research work concentrates on various aspects of computational fluid dynamics and heat transfer and application to a variety of engineering and environmental problems, including complex systems energy efficiency improvement using renewable technology integration, energy conservation and thermal insulation in buildings, application of nanofluids in heat transfer, data center cooling systems, adsorption cooling systems, and poly generation systems.

ZERYAB HASSAN KIANI received the B.E. degree in mechanical engineering from the National University of Sciences and Technology, Islamabad, Pakistan, in 2013, and the M.S. degree in power engineering from Technische Universität München (TUM), Munich, Germany, in in 2016. He has the IBM Certified Data Scientist. He is an experienced Renewable Energy Manager with a demonstrated history of working with Data in the renewables and environment industry. He has skilled in energy economy, solar industry, energy optimization, demand side management, and engineering software packages.

COLIN SOKOL KUKA (Graduate Student Member, IEEE) received the B.Sc. and M.Sc. degrees in electronics engineering from the University of Pisa, Italy, in 2011 and 2013, respectively. He is currently pursuing the Ph.D. degree with the University of York. He has more than five years working experience in industry worldwide with many applications of innovative products on the field. His research interests include security in wireless power transfer, memristor, artificial intelligence, and algorithms for energy management systems. He is a member of the Institution of Engineering and Technology (MIET). In 2014, he received the Information and Communications Technology (ICT) qualification from the Italian Order of Engineers.

● ● ●